

# Motion of charged particles on the Reissner-Nordström (Anti)-de Sitter black holes

Marco Olivares\*

*Departamento de Física, Facultad de Ciencia,  
Universidad de Santiago de Chile,  
Casilla 307, Santiago 2, Chile*

Joel Saavedra†

*Instituto de Física, Pontificia Universidad de Católica de Valparaíso,  
Av. Universidad 330, Curauma, Valparaíso, Chile*

J.R. Villanueva‡ and Carlos Leiva§

*Departamento de Física, Facultad de Ciencias,  
Universidad de Tarapacá,  
Av. General Velásquez 1775, Arica, Chile*  
(Dated: February 8, 2011)

In this work we address the study of movement of charged particles in the background of charged black holes with non-trivial asymptotic behavior. We compute the exact trajectories for massive-charged particles in terms of elliptic Jacobi functions. Finally we obtain a detailed description of orbits for Reissner-Nordström (Anti) de Sitter black holes in terms of charge, mass and energy of the particles.

PACS numbers: 04.20.Fy, 04.20.Jb, 04.40.Nr, 04.70.Bw

Keywords: Black Holes; Elliptic Functions.

## I. INTRODUCTION

Motion of particles on black holes is one interesting phenomena of classical gravity. At this respect, there are several studies about geodesic motion in the vicinity of black holes. For instance, the geodesic structure of the Schwarzschild (S), Reissner-Nordström (RN) and Kerr (K) black holes were studied in detail by Chandrasekhar [1]. There, the author studied motion of the test particles using the Lagrangian and the Newmann-Penrose formalism. If we think this problem in a modern point of view, it is of high interest to study the motion of particles in the vicinity of black holes with asymptotic behaviors others than the Schwarzschild case (flat case). Then, the so called SAdS or SdS black holes have been objects of highly consideration, due to the AdS-CFT conjecture, where there are powerful tools that relate gravitational theories with an asymptotically AdS behavior with a conformal field theories of one less dimension [2]. Besides, this kind of black holes provides a theoretical laboratory for understanding a lot of important points in black holes physics and gravity theories and their extensions. It is possible to generalize the asymptotic flat spacetimes by including a non-zero cosmological constant term. For instance, the Kotler solution [3] is obtained by imposing  $R_{\mu\nu} = \Lambda g_{\mu\nu}$  in the field equations. Some important implications of those can be found in [4, 5]. Different focuses in the research can be developed depending on the value of the cosmological constant: the Schwarzschild de Sitter case (SdS) (which is obtained by considering a positive value of the cosmological constant  $\Lambda > 0$ ), or the Schwarzschild anti-de Sitter case (SAdS) (which is obtained by considering a negative value of the cosmological constant, consider,  $\Lambda < 0$ ). There are some previous works about the geodesic motion in the SdS case [6–8]. On the other hand, when a negative cosmological constant,  $\Lambda < 0$ , is taking in to account i.e. Schwarzschild Anti de Sitter case (SAdS), the studies are more complicated. However different aspects of the geodesic structure of this spacetime can be found in [9–11]. The motion of (neutral) particles in RN black hole with non-zero cosmological constant has been studied in [12]. Furthermore, in Ref. [13–15], authors presented analytical solutions of the geodesic equation of massive test particles in higher dimensional Schwarzschild, Schwarzschild (anti) de Sitter ,S(A)dS, Reissner Nordström, RN, and Reissner Nordström (anti) de Sitter, RN(A)dS spacetimes and they obtained complete solutions and a classification

\*Electronic address: marco.olivares@usach.cl

†Electronic address: joel.saavedra@ucv.cl

‡Electronic address: jrvillanueva@uta.cl

§Electronic address: cleivas@uta.cl

of the possible orbits in these geometries in term of Weierstrass functions. Also, the equatorial circular motion in Kerr- de Sitter spacetime is studied in [16].

In this article we are interested in the study of the motion of charged particles on the Reissner-Nordström (Anti) de Sitter black hole. In doing so, we start considering the Hamilton-Jacobi formalism in order to write equations of motion and then we reduce our problem to quadratures. Then we solve quadratures equation and we found all the possible orbits for the geometries under consideration in terms of the elliptic Jacobi functions.

## II. MOTION OF CHARGED PARTICLES IN THE VICINITY OF BLACK HOLE

We are interested in the study of the motion of massive-charged particles near to an static, spherically symmetric and charged black hole when a non-zero cosmological constant is taken into account. The  $\Lambda > 0$  case is called the Reissner-Nordström de Sitter spacetime (RNDS), while the  $\Lambda < 0$  case is call it the Reissner-Nordström Anti de Sitter spacetime (RNAdS).

In terms of the usual Schwarzschild coordinates  $(t, r, \theta, \phi)$ , the metric is written as

$$ds^2 = -f(r)dt^2 + \frac{dr^2}{f(r)} + r^2(d\theta^2 + \sin^2\theta d\phi^2), \quad (1)$$

where  $f(r)$  is the lapsus function given by

$$f(r) = 1 - \frac{2M}{r} + \frac{Q^2}{r^2} - \frac{\Lambda r^2}{3}, \quad (2)$$

and the coordinates satisfy the relations:  $-\infty \leq t \leq \infty$ ,  $r \geq 0$ ,  $0 \leq \theta \leq \pi$  y  $0 \leq \phi \leq 2\pi$ .

We would like to consider the motion of test particles with mass  $m$  and charge  $q$  in the framework of general relativity. In order to obtain the equation of motion, we apply the Hamilton-Jacobi formalism. In this sense, the Hamilton-Jacobi equation for the geometry described by the metric  $g_{\mu\nu}$  is

$$g^{\mu\nu} \left( \frac{\partial S}{\partial x^\mu} + qA_\mu \right) \left( \frac{\partial S}{\partial x^\nu} + qA_\nu \right) + m^2 = 0, \quad (3)$$

where  $A_\mu$  represents the vector potential components associated with the charge of the black hole (because, we are considering charged static black holes where the only non-vanishing component of the vector potential is the temporal  $A_0 = \frac{Q}{r}$ ),  $S$  corresponds to the characteristic Hamilton function. Considering our metric this equation can be written as

$$-\frac{1}{f(r)} \left( \frac{\partial S}{\partial t} + \frac{qQ}{r} \right)^2 + f(r) \left( \frac{\partial S}{\partial r} \right)^2 + \frac{1}{r^2} \left( \frac{\partial S}{\partial \theta} \right)^2 + \frac{1}{r^2 \sin^2 \theta} \left( \frac{\partial S}{\partial \phi} \right)^2 + m^2 = 0, \quad (4)$$

in order to solve this equation we use the following ansatz

$$S = -Et + S_1(r) + S_2(\theta) + J\phi, \quad (5)$$

where  $E$  and  $J$  are identified as the energy and angular momentum of the particle. Using this ansatz Eq.(4) reads as follow

$$-\frac{r^2}{f(r)} \left( -E + \frac{qQ}{r} \right)^2 + r^2 f(r) \left( \frac{\partial S_1}{\partial r} \right)^2 + \left( \frac{\partial S_2}{\partial \theta} \right)^2 + J^2 \csc^2 \theta + r^2 m^2 = 0. \quad (6)$$

Using the standard procedure we recognize the following constant

$$L^2 = \left( \frac{\partial S_2}{\partial \theta} \right)^2 + J^2 \csc^2 \theta, \quad (7)$$

without lack of generality we consider that the motion is developed in the invariant plane  $\theta = \frac{\pi}{2}$  and in this case  $L$  is equal to angular momentum  $J$ . Then, we obtain the equation of motion

$$-\frac{r^2}{f(r)} \left( -E + \frac{qQ}{r} \right)^2 + r^2 f(r) \left( \frac{\partial S_1}{\partial r} \right)^2 + L^2 + r^2 m^2 = 0, \quad (8)$$

and thus, we find formal solutions for the radial component of the action

$$S_1(r) = \epsilon \int \frac{dr}{f(r)} \sqrt{\left(E - \frac{qQ}{r}\right)^2 - f(r) \left(m^2 + \frac{L^2}{r^2}\right)}, \quad (9)$$

where  $\epsilon = \pm 1$ . Now, using the Hamilton-Jacobi method, we simplify our study to the following quadrature problem

$$t = \epsilon \int \frac{dr}{f(r)} \left(E - \frac{qQ}{r}\right) \left[\left(E - \frac{qQ}{r}\right)^2 - f(r) \left(m^2 + \frac{L^2}{r^2}\right)\right]^{-1/2}, \quad (10)$$

where we can obtain the radial velocity to respect the coordinate time

$$\frac{dr}{dt} = \pm \frac{f(r)}{\left(E - \frac{qQ}{r}\right)} \sqrt{\left(E - \frac{qQ}{r}\right)^2 - f(r) \left(m^2 + \frac{L^2}{r^2}\right)}. \quad (11)$$

Now, the condition of turning point  $(\frac{dr}{dt})_{r=r_t} = 0$  allows us to define an effective potential. In fact, considering that

$$\frac{f(r)}{\left(E - \frac{qQ}{r}\right)} \neq 0, \forall r, \quad (12)$$

we can factorize the term under the square root as:

$$\left(E - \frac{qQ}{r}\right)^2 - f(r) \left(m^2 + \frac{L^2}{r^2}\right) = (E - V_-)(E - V_+), \quad (13)$$

where we can recognize the effective potential for the particle with mass  $m$  and electric charge  $q$  as

$$V_{\pm}(r) = \frac{qQ}{r} \pm \sqrt{f(r)} \sqrt{m^2 + \frac{L^2}{r^2}}, \quad (14)$$

therefore, eq.(11) can be written as

$$\frac{dr}{dt} = \pm \frac{f(r)}{\left(E - \frac{qQ}{r}\right)} \sqrt{[E - V_-(r)][E - V_+(r)]}. \quad (15)$$

Since the charge of the test particle is much smaller than the mass ( $q \ll M$ ), eventually  $V_- < 0$  and for this reason we choose the positive branch of the effective potential:  $V_{eff} = V_+ \equiv V$ . The behavior of effective potential is shown in Fig.1 for RNdS and RNAdS cases with different values of the angular momentum, but keeping  $m, q$  fixed. It's worth noting that the particle still has electric potential energy at the horizon.

Finally, we can classify different kinds of motion for massive-charged particles through the values of the  $L$  in the following way

- Motion of charged particles with angular momentum
- Motion of charged particles with vanishing angular momentum

In the following sections we study in detail the orbits before mentioned.

### A. Circular Orbits

The orbits can be classified by their values of energy and angular momentum. In order to have at least a stationary system the effective potential  $V(r)$  have to exhibit extremes for fixed values of radial coordinate,  $r = r_x$ ,

$$\frac{dV(r)}{dr}|_{r=r_x} = 0. \quad (16)$$

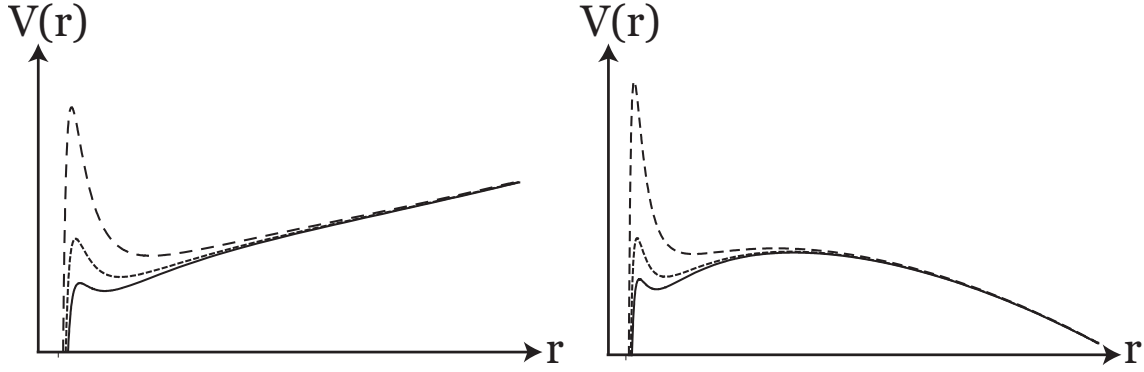


FIG. 1: Effective potential for charged particles on the geometry of RN for different values of angular momentum,  $L$  (left panel SAdS case and right panel SdS case). Both of them were plotted considering  $Q = 0.85M$ ,  $m = 0.2M$ ,  $q = 0.18M$  and  $\ell = 400M$ .

For simplicity, we rewrite the effective potential as

$$V(r) = h(r) + \sqrt{f(r) j(r)}, \quad (17)$$

where  $f(r)$  is the lapse function, and

$$h(r) = \frac{qQ}{r}, \quad j(r) = m^2 + \frac{L^2}{r^2}.$$

Therefore, using eq. (17) into eq. (16) yields

$$\left[ h'(r) \sqrt{f(r) j(r)} + \frac{1}{2} (f'(r) j(r) + f(r) j'(r)) \right]_{r=r_x} = 0 \quad (18)$$

Notice that this equation leads to a polynomial of twelfth grade, so, their solution is restricted to the numeric plane. However, it is possible to determine the periods of revolution of the circular orbits, both stable and unstable, with respect to the proper time,  $\tau$ , and coordinate time,  $t$ , in the following way: the condition (18) allows to obtain the angular momentum for the stable and unstable circle orbits,  $L_x = L_s$  and  $L_x = L_c$  (at  $r_x = r_s$  and  $r_x = r_c$  in FIG. 2, respectively; and  $r_x = r_e$  and  $r_x = r_i, R_i$  in FIG. 7, respectively). In our case, it is given by

$$a + b L_x^2 = [c + d L_x^2]^2, \quad (19)$$

where

$$a = m^2 f(r_x) h'(r_x)^2; \quad b = \frac{f(r_x) h'(r_x)^2}{r^2}; \quad c = \frac{m^2 f'(r_x)}{2}; \quad d = \frac{f'(r_x)}{2r^2} - \frac{f(r_x)}{r^3} \quad (20)$$

Thus, the real solution of the quadratic equation for  $L_x$  give us the angular momentum of the circular orbit. Explicitly, the constants of motion,  $L_x$  and  $E_x$ , for the circular orbits are given by

$$L_x = \left[ \frac{b - 2cd - \sqrt{b^2 + 4d(da - bc)}}{2d^2} \right]^{1/2}, \quad (21)$$

and

$$E_x = h(r_x) + \sqrt{f(r_x)} \left[ m^2 + \frac{b - 2cd - \sqrt{b^2 + 4d(da - bc)}}{2d^2 r^2} \right]. \quad (22)$$

Therefore, the proper period of the circular orbit ( $T_\tau = \frac{2\pi r_x^2}{L_x}$ ) is

$$T_\tau = 2\pi r_x^2 \left[ \frac{b - 2cd - \sqrt{b^2 + 4d(da - bc)}}{2d^2} \right]^{-1/2}, \quad (23)$$

and the coordinate period ( $T_t = \frac{2\pi r_x^2}{L_x f(r_x)} (E_x - h(r_x)) = T_\tau \sqrt{\frac{j(r_x)}{f(r_x)}}$ ) is

$$T_t = \frac{T_\tau}{\sqrt{f(r_x)}} \left[ m^2 + \frac{b - 2cd - \sqrt{b^2 + 4d(da - bc)}}{2d^2 r_x^2} \right]^{1/2}. \quad (24)$$

Notice that, if neutral particles are taken into account (i. e.  $q = 0$  and  $h(r_x) = 0$ ), the proper and coordinate period are given by

$$T_\tau = \frac{2\pi r_x}{m} \sqrt{\frac{r_x^2 - 3Mr_x + 2Q^2}{Mr_x - Q^2 - \Lambda r_x^4/3}}, \quad (25)$$

and

$$T_t = \frac{T_\tau}{\sqrt{f(r_x)}} \left[ \frac{r_x^2 - 2Mr_x + Q^2 - \Lambda r_x^4/3}{r_x^2 - 3Mr_x + 2Q^2} \right]^{1/2}, \quad (26)$$

respectively. Recently, the authors in [17] have studied other aspect of the circular motion of the neutral particles in the RN spacetime such as the stability of the orbits.

### III. CHARGED PARTICLES ON THE GEOMETRY OF REISSNER-NORDSTRÖM ANTI-DE SITTER BLACK HOLE

First at all, let's focus in the motion of charged particles on the geometry of Reissner-Nordström Anti-de Sitter black hole. In this case charged particles are affected by an effective potential described in right panel of Fig. 1. Considering motion with  $L \neq 0$  we obtain the equation

$$\dot{r}^2 = [E - V_-(r)][E - V(r)] = - \left( \frac{m}{\ell} \right)^2 \frac{P_6(r)}{r^4}, \quad (27)$$

where

$$P_6(r) = \sum_{j=0}^6 p_j r^j, \quad (28)$$

and the coefficients are

$$p_0 = \frac{Q^2 L^2 \ell^2}{m^2}, \quad p_1 = -\frac{2ML^2 \ell^2}{m^2}, \quad p_2 = \ell^2 \left( \frac{L^2}{m^2} + Q^2 - \frac{q^2 Q^2}{m^2} \right),$$

$$p_3 = -2\ell^2 \left( M - \frac{qQE}{m^2} \right), \quad p_4 = -\ell^2 \left( \frac{E^2}{m^2} - 1 - \frac{L^2}{m^2 \ell^2} \right), \quad p_5 = 0, \quad p_6 = 1.$$

The solutions (different and reals) of this sixth degree polynomial, correspond to the physical distance that characterize the motion for the so called periastron, apastron and circular orbit radii. Physical reality of orbits depends on the values of constants  $E, M, Q, q$  and  $L$ . We can distinguish in our description two sets of values for the constants in order to classify possible motions. One of them allows the existence of planetary orbits, in this case the polynomial has six real distances. Besides, this set has a second class trajectory that represents free fall to the event horizon. The second set of fixed values for the constants correspond to critical orbits, for example, here we have the unstable circle orbit. Finally, we discuss five trajectories that have physical meaning for the geometry under consideration (see FIG. 2 for a better visualization of the orbits.)

- **Planetary Orbit:** In this case the orbit corresponds to a bounded trajectory that exhibit oscillation between two extremal distances: the *periastron* and the *apastron*, ( $r_P$  and  $r_A$  in FIG. 2, respectively). For simplicity, we shall consider the case of a double-degenerate real negative root,  $\sigma_F$ , such that the polynomial  $P_6$  can be written as  $P_6(r) = (r - \sigma_F)^2 P_4(r)$ . This case has also a particular solution called Reissner-Nordström limit.
- **Second Kind Trajectory:** This trajectory is computed with the same parameter than the planetary orbits. It corresponds to a trajectory that starts at rest from a finite distance,  $r_F$ . This kind of motion represents the fall to the event horizon, and it is considered that has a turning point inside the Cauchy horizon,  $\rho_F$ .
- **Critical Trajectory:** There are trajectories of the first and second kind with angular momentum  $L_c$ , given by (??), and energy  $E_c$  given taken  $r = r_c$  in (13) and equating it to zero. The first one starts at rest at a finite distance outside from the unstable circular orbit,  $r_1$ , and then it approximates asymptotically to it. The second kind approximates to the unstable orbit from the inside of it.
- **Radial Trajectory:** These trajectories have null angular momentum and physically they describe radial fall from rest to the event horizon.
- **Circle Orbits:** For some fixed values of the constants it is possible to find solutions of the equation of motions that represent stable and unstable circle orbits. This case was discussed in the previous section and it is possible to find the connection with the Lyapunov exponent for the unstable orbit with the quasinormal modes [cardoso, work in progress].

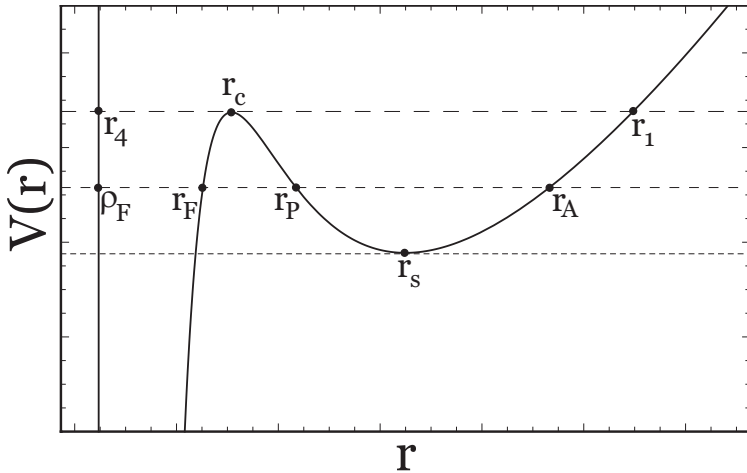


FIG. 2: Effective potential for charged particles on the geometry of RNAdS for  $M = 1$ ,  $Q = 0.85M$ ,  $\ell = 400M$ ,  $L = 0.33M^2$ ,  $q = 0.18M$  and  $m = 0.2M$ .

### A. Planetary Orbit

In order to characterize this motion we rewrite the polynomial  $P_4(r)$  in term of his roots

$$P_4(r) = (r - \rho_S)(r - r_S)(r - r_P)(r_A - r). \quad (29)$$

where  $\sigma_F < 0 < \rho_S < r_S < r_P < r_A$ , and we identify periastron and apastron distances as  $r_P$  and  $r_A$  respectively. These trajectories are defined inside the following limits  $r_P < r < r_A$ , and the equation of motion has the following quadrature

$$-\frac{dr}{d\phi} = \frac{\sqrt{P_6(r)}}{\ell L_P}, \quad (30)$$

where  $L_P$  is the angular momentum of the test particle in the planetary orbit. The corresponding integral is given by

$$\phi(r) = \ell L_P \int_{r_A}^r \frac{-dr}{(r - \sigma_F) \sqrt{P_4(r)}}, \quad (31)$$

now introducing constants  $\alpha_P = \frac{2\ell L_P}{\sqrt{(r_A - r_S)(r_P - \rho_S)}}$ ,  $\beta_P = \frac{1}{(\rho_S - \sigma_F)}$  y  $\gamma_P = -\frac{(r_A - \rho_S)}{(r_A - \sigma_F)(\rho_S - \sigma_F)}$ , it is possible to get the solution given by a Jacobi elliptic integrals of first and third kinds

$$\phi_P(r) = \phi_F^{(P)} + \phi_{\Pi}^{(P)}, \quad (32)$$

where  $\phi_F^{(P)} = \alpha_P \beta_P F(\psi_P; \kappa_P)$  and  $\phi_{\Pi}^{(P)} = \alpha_P \gamma_P \Pi(\psi_P; \kappa_P, n_P)$ , with the elliptic parameters given by

$$\psi_P = \arcsin \sqrt{\frac{(r_P - \rho_S)(r_A - r)}{(r_A - r_P)(r - \rho_S)}}, \quad (33)$$

$$\kappa_P = \sqrt{\frac{(r_A - r_P)(r_S - \rho_S)}{(r_A - r_S)(r_P - \rho_S)}}, \quad (34)$$

$$n_P = \frac{(r_P - r_A)(\sigma_F - \rho_S)}{(r_P - \rho_S)(\sigma_F - r_A)}, \quad (35)$$

similar results can be found in [13–15], where authors presented analytical solutions for the geodesic equation of massive test particles in higher dimensional Schwarzschild, Schwarzschild(anti)de Sitter, ReissnerNordstrom and ReissnerNordstrom(anti)de Sitter spacetimes. In FIG.3 we show orbits for an specific value of the angular momentum and present the case of an elliptic orbit that precesses between the periastron and apastron.

At this point, we can calculate the precession of the perihelion as

$$2\phi(r_P) = 2\pi + \Delta\varphi, \quad (36)$$

and considering the exact solution (32) we obtain

$$\Delta\varphi = 2 \left[ \phi_{\Pi}^{(P)}(r_P) + \phi_F^{(P)}(r_P) \right] - 2\pi, \quad (37)$$

One particular solution is obtained, when we perform a fine tuning in the physical distance under consideration. This case corresponds to the called Reissner-Nordström limit, that we are going to discuss in the next subsection.

### 1. Reissner-Nordström Limit

One approximated solution of the first order represents the limit case of the motion on Reissner-Nordström black hole. This limit corresponds to the solution when  $\ell \rightarrow \infty$  and therefore we must consider the potential

$$V(r) = \frac{qQ}{r} + \sqrt{\left(1 - \frac{2M}{r} + \frac{Q^2}{r^2}\right) \left(m^2 + \frac{L^2}{r^2}\right)},$$

in which case we obtain two kinds of orbits:

- confined orbits: they are obtained when the relation  $E < m$  is satisfied.

- non-confined orbits: they are obtained when the relation  $E \geq m$  is satisfied.

i).- Confined orbits: defining  $\zeta^2 = (m^2 - E^2)^{-1}$ , the motion equation (30) can be written as

$$\left(\frac{dr}{d\phi}\right)^2 = \frac{P_4(r)}{\zeta^2 L^2},$$

where,

$$P_4(r) = \sum_{j=0}^4 p'_j r^j$$

and the coefficients are

$$p'_0 = -\zeta^2 Q^2 L^2; \quad p'_1 = 2\zeta^2 M L^2; \quad p'_2 = -\zeta^2 (L^2 + m^2 Q^2 - q^2 Q^2); \quad p'_3 = 2\zeta^2 (m^2 M - q Q E); \quad p'_4 = -1,$$

In terms of the roots of the polynomial, we can write

$$p'_4 = (r'_A - r)(r - r'_P)(r - r'_F)(r - \rho'_F).$$

Then, the solution can be written as

$$\phi'_P(r) = \alpha'_P F(\psi'_P; \kappa'_P)$$

where

$$\alpha'_P = \frac{2\zeta L'}{(\sqrt{r'_A - r'_F})(r'_P - \rho'_F)};$$

$$\psi'_P = \arcsin \sqrt{\frac{(r'_P - \rho'_F)(r'_A - r)}{(r'_A - r'_P)(r - \rho'_F)}}$$

$$\kappa'_P = \sqrt{\frac{(r'_A - r'_P)(r'_F - \rho'_F)}{(r'_A - r'_F)(r'_P - \rho'_F)}}$$

Defining the constants  $\varpi = \frac{1}{\alpha'_P}$  and  $\delta = \frac{(r'_A - r'_P)}{(r'_P - \rho'_F)}$ , we can write the solution in terms of elliptic Jacobi sine

$$r(\phi') = \frac{r'_A + \rho'_F \delta \operatorname{sn}^2(\varpi \phi')}{1 + \delta \operatorname{sn}^2(\varpi \phi')}, \quad (38)$$

In our case, the precession of the perihelion (36) is given by

$$\Delta\varphi = 2[\alpha'_P K(\kappa'_P) - \pi], \quad (39)$$

where  $K(\kappa'_P)$  is the complete elliptic Jacobi integral of the first kind.

## B. Second Kind Trajectory

This trajectory corresponds to the one where the test particle starts at rest from a finite distance bigger than the event horizon and then falls to it. Its motion is developed in the following region  $\rho_S < r < r_S$ . In this case the corresponding angular quadrature is given by

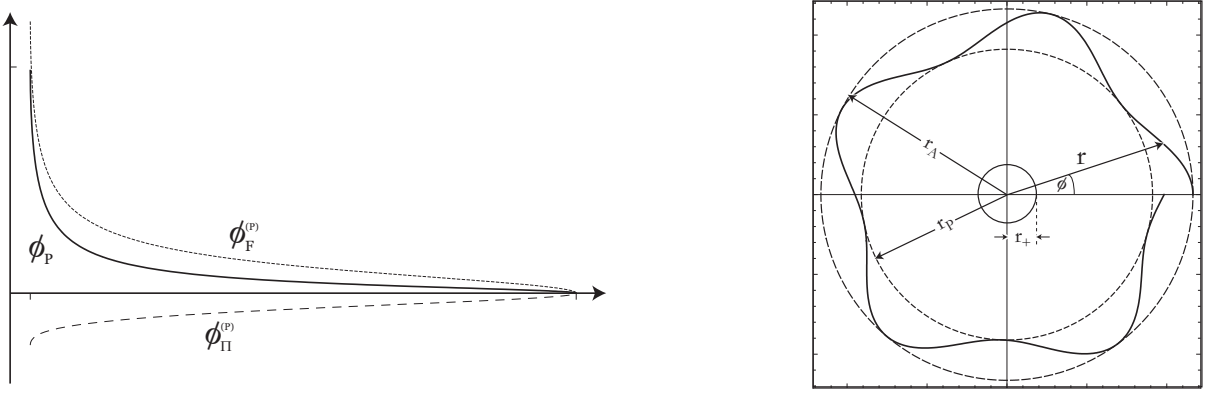


FIG. 3: Polar plot for the planetary orbit of the test particle in the Reissner-Nordström Limit. Clearly, there is a precession of the perihelion, which is given explicitly by eq.(39).

$$\phi(r) = \ell L_P \int_{r_S}^r \frac{-dr}{(r - \sigma_F) \sqrt{P(r)}}, \quad (40)$$

now we have a fourth degree polynomial described by

$$P(r) = (r - \rho_S)(r_S - r)(r_P - r)(r_A - r). \quad (41)$$

Using a similar procedure than the used for the planetary orbit, we first define the following constants  $\alpha_s = \frac{2\ell L_P}{\sqrt{(r_A - r_S)(r_P - \rho_S)}} = \alpha_P$ ,  $\beta_s = \frac{1}{r_P - \sigma_F}$  and  $\gamma_s = \frac{r_P - r_S}{(\sigma_F - r_P)(\sigma_F - r_S)}$ . The solution can be written in terms of Jacobi elliptic functions as follows

$$\phi_s(r) = \phi_F^{(s)} + \phi_{\Pi}^{(s)}, \quad (42)$$

where  $\phi_F^{(s)} = \alpha_s \beta_s F(\psi_s; \kappa_s)$  and  $\phi_{\Pi}^{(s)} = \alpha_s \gamma_s \Pi(\psi_s; \kappa_s, n_s)$ , with

$$\psi_s = \arcsin \sqrt{\frac{(r_P - \rho_S)(r_S - r)}{(r_S - \rho_S)(r_P - r)}}, \quad (43)$$

$$\kappa_s = \sqrt{\frac{(r_A - r_P)(r_S - \rho_S)}{(r_A - r_S)(r_P - \rho_S)}} = \kappa_P, \quad (44)$$

$$n_s = \frac{(r_S - \rho_S)(\sigma_F - r_P)}{(r_P - \rho_S)(\sigma_F - r_S)}, \quad (45)$$

This kind of trajectory is shown in Fig.(4) where we show the analytic continuation to the inner space to the event horizon. In sum this trajectories are doomed to cross the event horizon.

### C. critical trajectory

There are trajectories of the first and second kind. The first one starts at rest at a finite distance outside from the unstable circular orbit and then it approximates asymptotically to it. The second kind approximates to the unstable orbit from inner distance.

### 1. First class critical trajectory

Critical trajectory of the first kind corresponds to the motion of particles to asymptotically tend to a circle orbit from a great distance compared to the radius of this orbit. The region of this motion is defined by the limits  $r_c < r < r_1$  and the respective polynomial becomes

$$F_c(r) = (r - r_6)(r - r_5)(r - r_4)(r - r_c)^2(r_1 - r). \quad (46)$$

then we can obtain the integral for the orbit as follows

$$\phi_c^{(1)}(r) = \ell L_P \int_{r_1}^r \frac{-dr}{(r - r_c)\sqrt{(r_1 - r)(r - r_4)(r - r_5)(r - r_6)}}. \quad (47)$$

Defining the following constants  $\alpha_1 = \frac{2\ell L_P}{\sqrt{(r_1 - r_5)(r_4 - r_6)}}$ ,  $\beta_1 = \frac{1}{(r_6 - r_c)}$  and  $\gamma_1 = \frac{(r_6 - r_1)}{(r_1 - r_c)(r_6 - r_c)}$  we can obtain a solution for polar angle

$$\phi_c^{(1)}(r) = \phi_F^{(1)}(r) + \phi_{\Pi}^{(1)}(r), \quad (48)$$

where the angles  $\phi_F^{(1)}(r)$  and  $\phi_{\Pi}^{(1)}(r)$  are given in terms of the elliptic Jacobi integrals of the first and third kind,

$$\phi_F^{(1)}(r) = \alpha_1 \beta_1 F(\psi_c; \kappa_c), \quad \phi_{\Pi}^{(1)}(r) = \alpha_1 \gamma_1 \Pi(\psi_c; \kappa_c, n_c), \quad (49)$$

respectively, where their parameters are

$$\psi_c^{(1)}(r) = \arcsin \sqrt{\frac{(r_4 - r_6)(r_1 - r)}{(r_1 - r_4)(r - r_6)}}, \quad (50)$$

$$\kappa_c^{(1)} = \sqrt{\frac{(r_1 - r_4)(r_5 - r_6)}{(r_1 - r_5)(r_4 - r_6)}}, \quad (51)$$

and

$$n_c^{(1)} = \frac{(r_6 - r_c)(r_4 - r_1)}{(r_1 - r_c)(r_4 - r_6)}. \quad (52)$$

In FIG. 4 we plot the polar angle,  $\phi_c^{(1)}$ , as a function of the radial coordinate,  $r$ . We can see that  $\phi_{\Pi}^{(1)}$  dominates the behavior of  $\phi_c^{(1)}$  along the trajectory, specially when  $r \rightarrow r_c$ , in which case  $\phi_F^{(1)}$  takes a finite value. This trajectory is

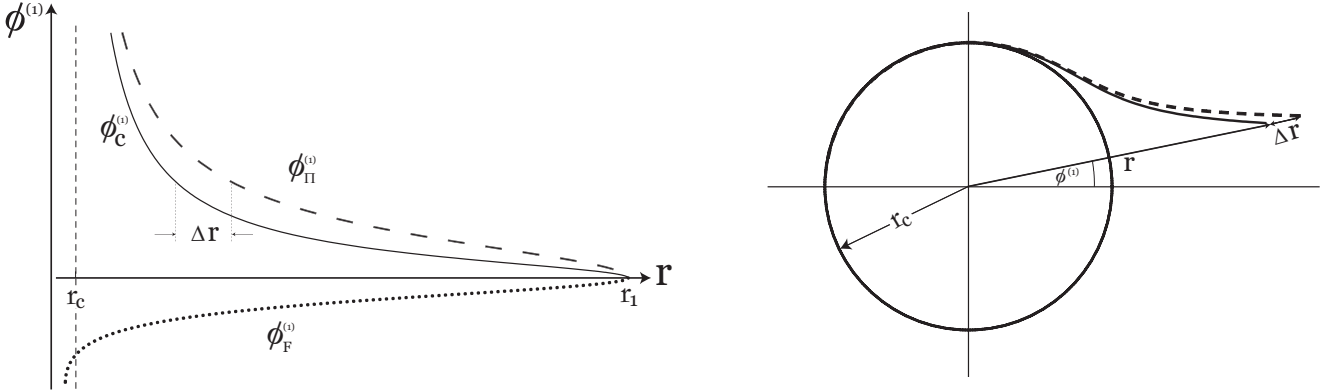


FIG. 4: Plot of the polar angle,  $\phi_c^{(1)}$ , as a function of the radial coordinate,  $r$ , with  $M = 1$ ,  $Q = 0.85M$ ,  $\ell = 10M$ ,  $L = 9M^2$ ,  $q = 0.18M$  and  $m = 0.2M$

characterized by an asymptotic tendency to the unstable circle orbit from distance bigger than the circle orbit radius *i.e.* in a infinite time we can found the particle in such orbit.

## 2. Second class critical trajectory

In this case particles asymptotically tend to the circle orbit from a distance less than the critical and the motion is realized in the following range  $r_4 < r < r_c$ . Then, we start considering  $\alpha_1$  (as was defined in previous case), the constant  $\beta_2 = \frac{1}{(r_c - r_5)}$  and  $\gamma_2 = \frac{(r_4 - r_5)}{(r_c - r_4)(r_c - r_5)}$ , therefore our solution is written as

$$\phi_c^{(2)}(r) = \alpha_1 [\beta_2 F(\psi_c; \kappa_c) + \gamma_2 \Pi(\psi_c; \kappa_c, n_c)], \quad (53)$$

where

$$\psi_c^{(2)} = \arcsin \sqrt{\frac{(r_1 - r_5)(r - r_4)}{(r_1 - r_4)(r - r_5)}}, \quad (54)$$

$$\kappa_c^{(2)} = \sqrt{\frac{(r_1 - r_4)(r_5 - r_6)}{(r_1 - r_5)(r_4 - r_6)}}, \quad (55)$$

and

$$n_c^{(2)} = \frac{(r_5 - r_c)(r_1 - r_4)}{(r_4 - r_c)(r_1 - r_5)}, \quad (56)$$

As in the last case the motion asymptotically tends to the unstable circular orbit. For example in FIG. 5 we show the possible motion starting from a distance less than the one corresponding to the unstable circular orbit and tending to it.

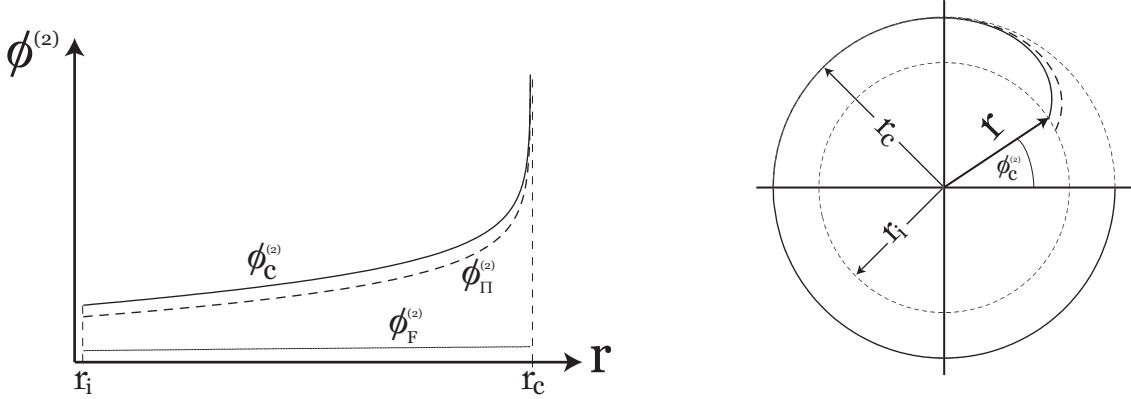


FIG. 5: Second class critical trajectory

## IV. RADIAL TRAJECTORIES

Radial motion corresponds to a trajectory with vanished angular momentum. First at all, we are considering the case of background of RNAdS, where  $Q < M$ . Let us start with the relation

$$\frac{1}{f(r)} = \ell^2 \frac{r^2}{F(r)}, \quad (57)$$

where the fourth degree polynomial is given by  $F(r) = r^4 + \ell^2(r^2 - 2Mr + Q^2) = (r - r_+)(r - r_-)j(r)$ . Now the dynamical behavior is governed by

$$\left( \frac{dr}{d\tau} \right)^2 = \left( E - \frac{qQ}{r} \right)^2 - m^2 \left( 1 - \frac{2M}{r} + \frac{Q^2}{r^2} + \frac{r^2}{\ell^2} \right), \quad (58)$$

then, the trajectory equation can be written in the following form

$$\left(\frac{dr}{d\tau}\right)^2 = \frac{m^2}{\ell^2} \frac{G(r)}{r^2}, \quad (59)$$

where we define the fourth degree polynomial  $G(r) \equiv \sum_{j=0}^4 \alpha_j r^j$ , with the coefficients  $\alpha_0 = -Q^2 \ell^2 (1 - q^2/m^2)$ ,  $\alpha_1 = 2\ell^2(M - qQE/m^2)$ ,  $\alpha_2 = \ell^2(E^2/m^2 - 1)$ ,  $\alpha_3 = 0$  and  $\alpha_4 = -1$ . The proper time quadrature is

$$\tau(r) = \pm \frac{\ell}{m} \int \frac{r}{\sqrt{G(r)}} dr, \quad (60)$$

this motion corresponds to the radial fall starting at rest from the distance  $R_0$ . Then, considering negative sign, the radial function in this case is written as  $G(r) = (R_0 - r)(r - \rho_0)(r - \sigma_1)(r - \sigma_2)$ , whose four real roots are  $R_0 > r > \rho_0 > 0 > \sigma_1 > \sigma_2$ . Then we can write our solution as follows

$$\tau(r) = k_0 \Pi(\Psi; \kappa, \nu) + k_I F(\Psi; \kappa), \quad (61)$$

where

$$k_0 = \frac{\ell}{m} \frac{2(R_0 - \sigma_2)}{\sqrt{(R_0 - \sigma_1)(\rho_0 - \sigma_2)}}, \quad (62)$$

$$k_I = \frac{\ell}{m} \frac{2\sigma_2}{\sqrt{(R_0 - \sigma_1)(\rho_0 - \sigma_2)}}. \quad (63)$$

$$\Psi = \arcsin \sqrt{\frac{(\rho_0 - \sigma_2)(R_0 - r)}{(R_0 - \rho_0)(r - \sigma_2)}}, \quad (64)$$

$$\kappa = \sqrt{\frac{(R_0 - \rho_0)(\sigma_1 - \sigma_2)}{(R_0 - \sigma_1)(\rho_0 - \sigma_2)}}, \quad (65)$$

and

$$\nu = \frac{\rho_0 - R_0}{\rho_0 - \sigma_2}, \quad (66)$$

are constants. On the other hand, the corresponding coordinate time quadrature is given by

$$t(r) = \frac{\ell^3}{m} \int_{R_0}^r \left( \frac{Er^3 - qQr^2}{F(r)} \right) \frac{-dr}{\sqrt{G(r)}}, \quad (67)$$

in order to see physical contents, it is necessary to separate in partial fractions the term under the integral,

$$\frac{Er^3 - qQr^2}{F(r)} = \frac{A}{r - r_+} + \frac{B}{r - r_-} + \frac{C + Dr}{j(r)}, \quad (68)$$

where function  $j(r) = r^2 + ar + b^2$ , and the constant are given by  $a = r_- + r_+$  y  $b^2 = \ell^2 + a^2 - r_- r_+$ . One important point is the physical behavior of the coordinate time near the event horizon. There, the leading term is of the first order, where the constant is  $A = \frac{r_+^2(Er_+ - qQ)}{(r_+ - r_-)j(r_+)}$ . Therefore we can write the general solution in this case as

$$t(r) = A_0 t_D(r) + A_1 t_1(r) + A_2 t_2(r) + A_3 t_3(r). \quad (69)$$

There, we can see that near horizon the coordinate term is given by the leading term

$$t(r) \approx A_0 t_D(r), \quad (70)$$

where the constant is

$$A_0 = \frac{\ell^3}{m} \frac{2A}{(R_0 - r_+)(r_+ - \sigma_2)\sqrt{(R_0 - \sigma_1)(\rho_0 - \sigma_2)}}, \quad (71)$$

the exact solution for this term at the event horizons is

$$t_D(r) = (R_0 - \sigma_2)\Pi(\Psi; \kappa, n) - (R_0 - r_+)F(\Psi; \kappa), \quad (72)$$

where this solution is defined with the same set of parameters than the proper time solution, but just we are added the constant

$$n = \nu \frac{r_+ - \sigma_2}{r_+ - R_0}, \quad (73)$$

FIG. 6, shows the behavior for the proper and coordinate time. In simples terms, these solutions are very similar to Schwarzschild case where in the proper time framework particles can cross the event horizon and for the coordinate time framework, event horizon acts as an asymptotic line.

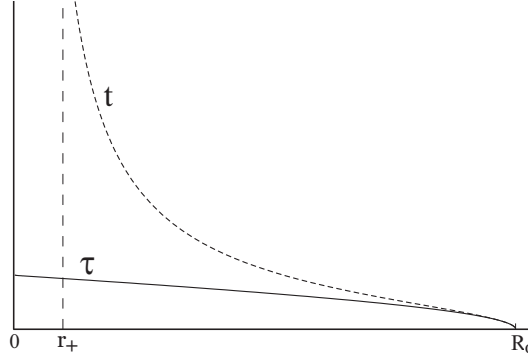


FIG. 6: Radial motion of the test particle for the proper time,  $\tau$  (solid curve), and the coordinate time,  $t$  (dashed curve). These solutions are very similar to Schwarzschild case where in the proper time framework particles can cross the event horizon and in the coordinate time framework, event horizon acts as an asymptotic line. Both curves are plotted by using  $m = 0.05M$ ,  $Q = 0.85M$ ,  $q = 0.01M$ ,  $\ell = 23M$ ,  $E = 0.067M$

## V. MOTION OF CHARGED PARTICLES ON THE REISSNER-NORDSTRÖM DE SITTER BLACK HOLE

In a similar way than the previous case of the RNAdS black hole, we start with particles with angular momentum  $L \neq 0$ , then radial quadrature is given by

$$\left( \frac{dr}{d\tau} \right)^2 = [E - V_-(r)] [E - V(r)], \quad (74)$$

then we can write the basic equation of the trajectories as follows ( $\Lambda/3 \equiv 1/\lambda^2 > 0$ )

$$\dot{r}^2 = \left( \frac{m}{\lambda} \right)^2 \frac{P_6(r)}{r^4}, \quad (75)$$

where the characteristic polynomial for the allowed trajectories is

$$P_6(r) = \sum_{j=0}^6 \omega_j r^j, \quad (76)$$

the coefficients are given by

$$\omega_0 = -\frac{\lambda^2 Q^2 L^2}{m^2}, \quad \omega_1 = \frac{2\lambda^2 M L^2}{m^2}, \quad \omega_2 = -\lambda^2 \left( \frac{L^2}{m^2} + Q^2 - \frac{q^2 Q^2}{m^2} \right),$$

$$\omega_3 = 2\lambda^2 \left( M - \frac{qQE}{m^2} \right), \quad \omega_4 = \lambda^2 \left( \frac{E^2}{m^2} - 1 + \frac{L^2}{m^2\lambda^2} \right), \quad \omega_5 = 0, \quad \omega_6 = 1.$$

Using the constant  $\zeta = \frac{\lambda L}{m}$ , we can write the angular quadrature as

$$\phi(r) = \pm \zeta \int^r \frac{dr}{\sqrt{P_6(r)}}, \quad (77)$$

Now we will give a detailed description of trajectories as in the previous case. First we need to define the kind of motion in terms of his energy and angular momentum against the effective potential.

- Orbit with angular momentum: here we have, for a specific combination of energy and angular momentum, the possibility to have planetary orbits, when the effective potential exhibits a minimum. Besides, we have three different kinds of orbits that depend on the energy of the particle, compared to the effective potential. The first kind orbits take place between the two maxima (that is planetary orbits). The second kind orbits have the same energy than those from the first kind, but they fall to the event horizon,  $r_+$ . Third kind orbits are those with the same energy than the cases before, but they instead fall to the cosmological horizon.  $r_{++}$ .
- Radial Orbit ( $L = 0$ ) this orbit corresponds to a free fall to cosmological horizon or event horizon.

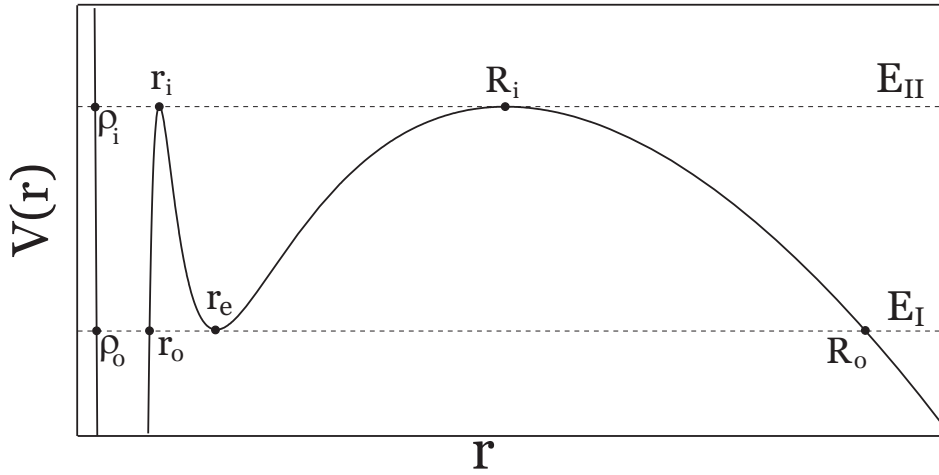


FIG. 7: Effective potential for charged particles on the geometry of RNdS for  $M = 1$ ,  $Q = 0.85M$ ,  $\ell = 400M$ ,  $L = 0.33M^2$ ,  $q = 0.18M$  and  $m = 0.2M$ .

#### A. Second Kind trajectory: Fall to event horizon

In the de Sitter case there are trajectories that start from a finite distance, at rest, and fall to the event horizon. The motion is developed in the region  $r_0 \geq r \geq r_+ > \rho_0$ . From (77) with the negative sign and the characteristic polynomial  $P_6(r) = (R_0 - r)(r_e - r)^2(r_0 - r)(r - \rho_0)(r - \sigma_0)$  we obtain the integral motion as follows,

$$\phi(r) = \zeta \int_{r_0}^r \frac{-dr}{(r_e - r)\sqrt{(R_0 - r)(r_0 - r)(r - \rho_0)(r - \sigma_0)}}. \quad (78)$$

Therefore the solution can be written as

$$\frac{1}{\zeta} \phi(r) = \alpha_s [\beta_s F(\varphi; k_s) + \gamma_s \Pi(\varphi; k_s, n_s)], \quad (79)$$

where the constants are given by  $\alpha_s = \frac{2}{\sqrt{(R_0 - \rho_0)(r_0 - \sigma_0)}}$ ,  $\beta_s = \frac{1}{(r_e - R_0)}$  and  $\gamma_s = \frac{(R_0 - r_0)}{(R_0 - r_e)(r_e - r_0)}$ . Also the parameters of the elliptic integrals are

$$k_s = \sqrt{\frac{(r_0 - \rho_0)(R_0 - \sigma_0)}{(R_0 - \rho_0)(r_0 - \sigma_0)}}, \quad n_s = \frac{(r_0 - \rho_0)(r_e - R_0)}{(R_0 - \rho_0)(r_e - r_0)}, \quad \text{and} \quad \varphi(r) = \arcsin \sqrt{\frac{(R_0 - \rho_0)(r_0 - r)}{(r_0 - \rho_0)(R_0 - r)}}, \quad (80)$$

Fig.(8) shows us allowed trajectories of the charged particles in this case. Here, we can observe that the trajectories starting from a distances bigger than event horizon are doomed to cross it and fall to singularity.

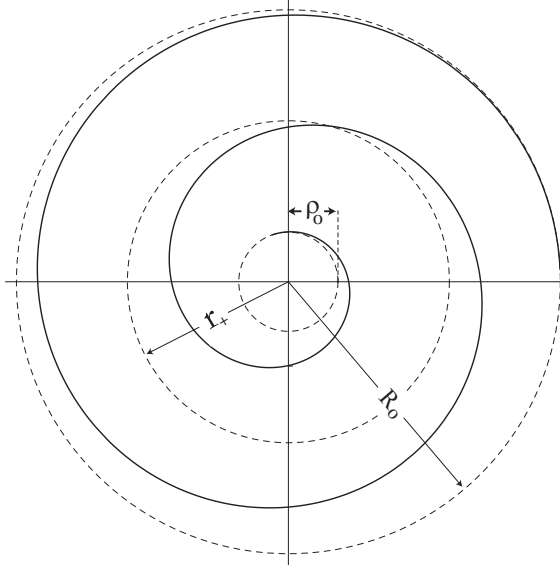


FIG. 8: Second Kind motion: It corresponds to trajectory starting from a distances bigger than event horizon are doomed to cross it and fall to singularity.

### B. Third Kind Trajectory: Fall to cosmological horizon

This case corresponds to the motion that starts at a finite distance from the event horizon and moves out from the field forces, crossing the cosmological horizon. In this case the allowed range is given by  $r \geq R_0$ . Integral Quadrature is

$$\phi(r) = \zeta \int_{R_0}^r \frac{dr}{(r - r_e) \sqrt{(r - R_0)(r - r_0)(r - \rho_0)(r - \sigma_0)}}, \quad (81)$$

again the solution can be written in terms of elliptical Jacobi integrals

$$\frac{1}{\zeta} \phi(r) = \alpha_t [\beta_t F(\varphi; k_t) + \gamma_t \Pi(\varphi; k_t, n_t)], \quad (82)$$

where the constants are given by  $\alpha_t = \frac{2}{\sqrt{(R_0 - \rho_0)(r_0 - \sigma_0)}}$ ,  $\beta_t = \frac{1}{(r_0 - r_e)}$  and  $\gamma_t = \frac{(R_0 - r_0)}{(R_0 - r_e)(r_e - r_0)}$ , and the corresponding elliptic parameters are

$$k_t = \sqrt{\frac{(r_0 - \rho_0)(R_0 - \sigma_0)}{(R_0 - \rho_0)(r_0 - \sigma_0)}}, \quad (83)$$

$$n_t = \frac{(R_0 - \sigma_0)(r_e - r_0)}{(r_0 - \sigma_0)(r_e - R_0)}, \quad (84)$$

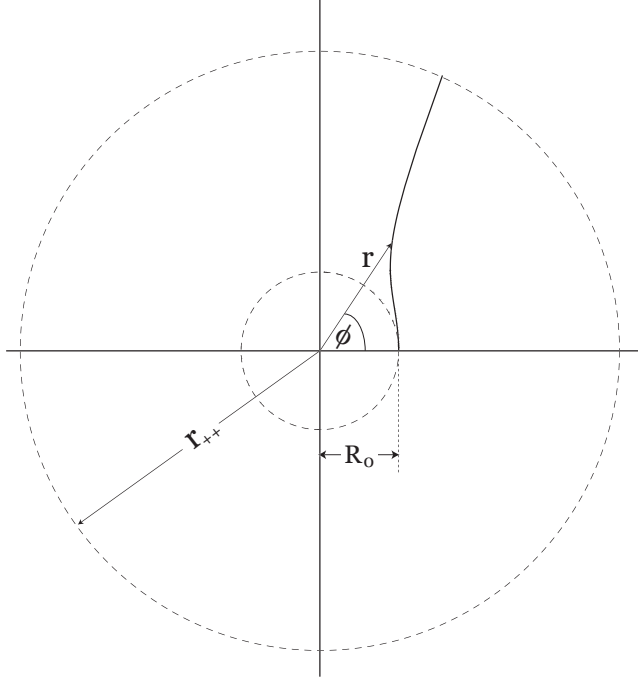


FIG. 9: Third Kind motion for a RNdS geometry: the particles moving out from the event horizon and then they are able to cross the cosmological horizon losing casual connection with physical observers.

$$\psi(r) = \arcsin \sqrt{\frac{(r_0 - \sigma_0)(r - R_0)}{(R_0 - \sigma_0)(r - r_0)}}, \quad (85)$$

FIG.9 depicts these trajectories, that correspond to particles moving out from the event horizon and then they are able to cross the cosmological horizon losing casual connection with physical observers.

### C. Critical Trajectory

As we have say, it is possible to obtain a class of orbits which posses two maxima at  $r_i$  and  $R_i$  ( $r_i < R_i$ ) with the same value of the constant  $E \equiv E_{II}$  (see FIG.7). In this case, the conditions

$$V(r_i) = V(R_i) \equiv E_{II}, \quad (86)$$

and

$$\left( \frac{dV(r)}{dr} \right)_{r=R_i} = \left( \frac{dV(r)}{dr} \right)_{r=r_i} = 0, \quad (87)$$

are satisfied. In this scenario, we can identify three possible trajectories: particles falling from an initial distance,  $d_1$  ( $d_1 < r_{++}$ ), to the unstable circular orbit at  $R_i$  (first kind critical orbit); another one goes up to the unstable circular orbit at  $r_i$  (second kind critical orbit) from an initial distance,  $d_2$  ( $d_2 > r_+$ ); and finally, the particles going to an asymptotically circular orbits at  $R_i$  or  $r_i$  (third kind critical orbit) depending on the sign of its initial velocity. Thus, the - (+) sign means that the particles falls (up) to the asymptotic orbit at  $r_i$  ( $R_i$ ).

#### 1. first kind critical orbit

In this case, the particle starts its motion at  $d_1$  and falls to the asymptotic orbit at  $R_i$ . From (77) with the negative sign and the characteristic polynomial given by  $P_6(r) = (r - R_0)^2(r - r_i)^2(r - \rho_i)(r - \sigma_i)$ , we obtain the solution

$$\phi_c^{(1)}(r) = \frac{\zeta}{\eta(R_i, r_i)} \left[ \frac{1}{\xi(R_i)} \ln \Theta(r, R_i) - \frac{1}{\xi(r_i)} \ln \Theta(r, r_i) \right], \quad (88)$$

where

$$\Theta(u, v) = 2\xi(v) \left( \frac{\xi(u) + \xi(v)}{\eta(u, v)} \right) + \eta(v, \rho_i) + \eta(v, \sigma_i), \quad (89)$$

with

$$\eta(u, v) = u - v, \quad \text{and} \quad \xi(u) = \sqrt{\eta(u, \rho_i) \eta(u, \sigma_i)}. \quad (90)$$

In left panel of FIG. 10 we have shown a typical first kind trajectory.

### 2. second kind critical orbit

This orbits have trajectories that go up asymptotically to the unstable circular orbit at  $r_i$  from a distance  $d_2$  ( $d_2 > r_+$ ). Thus, we must choose the plus sign in eq. (77) with the characteristic polynomial given by  $P_6(r) = (R_i - r)^2(r_i - r)^2(r - \rho_i)(r - \sigma_i)$ , in which case we obtain the solution

$$\phi_c^{(2)}(r) = -\frac{\zeta}{\eta(R_i, r_i)} \left[ \frac{1}{\xi(R_i)} \ln(-\Theta(r, R_i)) - \frac{1}{\xi(r_i)} \ln(-\Theta(r, r_i)) \right], \quad (91)$$

that we show in middle panel of FIG. 10.

### 3. third kind critical orbit

Finally, when the particle is at an initial distance  $d_3$ , such that  $r_i \leq d_3 \leq R_i$ , it has the ability to go asymptotically to the unstable circular orbit at  $r_i$  or  $R_i$ , depending on the sign of its initial velocity. Therefore, the solution can be write as

$$\phi_c^{(3)}(r) = \pm \frac{\zeta}{\eta(R_i, r_i)} \left[ \frac{1}{\xi(R_i)} \ln(-\Theta(r, R_i)) + \frac{1}{\xi(r_i)} \ln \Theta(r, r_i) \right] - \vartheta_0, \quad (92)$$

where  $\vartheta_0$  is a constant of integration that fixes the initial conditions and the - (+) sign means that the particle approaches to the unstable circular orbit at  $r_i$  ( $R_i$ ). In right panel of FIG. 10 we show this trajectories.

## VI. RADIAL MOTION

The motion of radial particles ( $L = 0$ ) is described by the equation

$$\left( \frac{dr}{d\tau} \right)^2 = \left( E - \frac{qQ}{r} \right)^2 - m^2 \left( 1 - \frac{2M}{r} + \frac{Q^2}{r^2} - \frac{\Lambda r^2}{3} \right). \quad (93)$$

The effective potential in this case is showed in

For different values of the constant of motion  $E$ , we have the following allowed orbits: The capture zone ( $E < E_c$ ) and critical motion ( $E = E_c$ ).

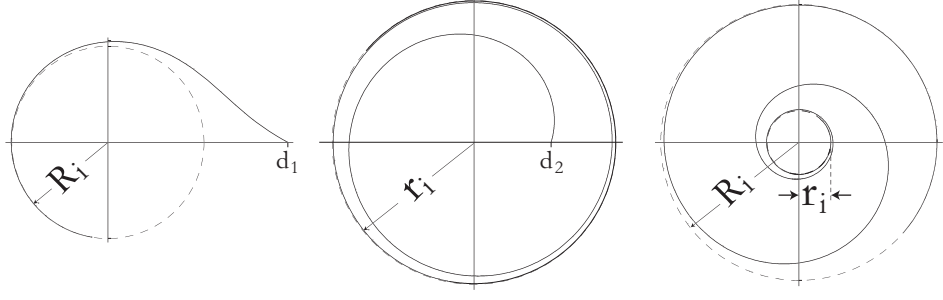


FIG. 10: Critical trajectories for charged particles in RNdS spacetime. Left panel: First kind orbit. The particle starts its motion from  $d_1$  ( $\phi_c^{(1)} = 0$ ) and approaches asymptotically to unstable circular orbit at  $R_i$ ; Middle panel: Second kind orbit. The particle starts its motion from  $d_2$  ( $\phi_c^{(2)} = 0$ ) and approaches asymptotically to unstable circular orbit at  $r_i$ . Right panel: Third kind orbit. The particle goes to the unstable circular orbit at  $r_i$  or  $R_i$ , depending on the sign of its initial velocity; All graphics has been plotted using  $M = 1$ ,  $m = 0.1M$ ,  $Q = 0.85M$ ,  $q = 0.01M$ ,  $\lambda = 400M$

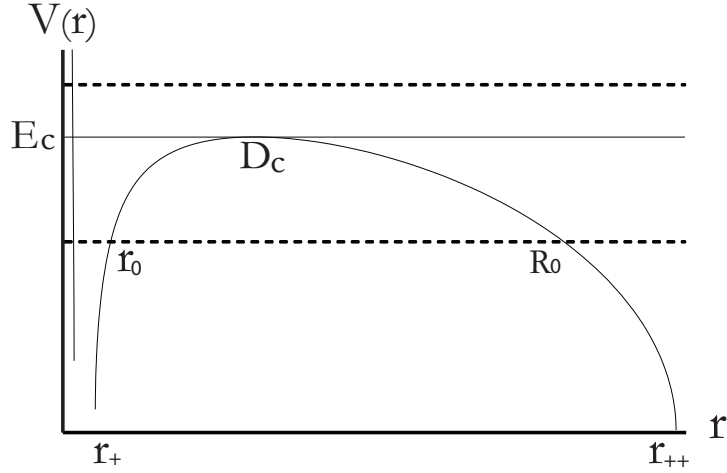


FIG. 11: Effective potential for radial charged particles in the RNdS spacetime with  $m = 0.1$ ,  $M = 1$ ,  $Q = 0.8$ ,  $q = 0.01$ ,  $\Lambda = 400M$

### A. Capture Zone

In this case, we have that  $E < E_c$ , and from here, we study two kind of orbits: first kind orbit, which fall to the cosmological horizon, and second kind orbit, which fall to the event horizon. It is convenient to rewrite eq. (93) in the form

$$\left( \frac{dr}{d\tau} \right)^2 = \frac{m^2}{\lambda^2} \frac{G(r)}{r^2}, \quad (94)$$

where the characteristic polynomial is

$$G(r) = r^4 - \alpha r^2 + \beta r - \gamma, \quad (95)$$

and the constants are given by  $\alpha = \lambda^2(1 - E^2/m^2)$ ,  $\beta = 2\lambda^2(M - qQE/m^2)$  and  $\gamma = \lambda^2Q^2(1 - q^2/m^2)$ .

Finally, we have the following relations in order to obtain the motion integrals

$$\pm \frac{dr}{d\tau} = \frac{m}{\lambda} \frac{\sqrt{G(r)}}{r}, \quad (96)$$

$$\pm \frac{dt}{d\tau} = \lambda^2 \frac{r^2}{F(r)} \left( E - \frac{qQ}{r} \right), \quad (97)$$

$$\pm \frac{dr}{dt} = \frac{m}{\lambda^3} F(r) \left( E - \frac{qQ}{r} \right)^{-1} \frac{\sqrt{G(r)}}{r^3}. \quad (98)$$

### 1. First Kind: Fall to event horizon

Radial motion shows more variety depending on the roots of the respective polynomial and the energy of the particles. This case corresponds to particles that start from a finite distance bigger than the last root of the effective potential and less than cosmological horizon. Here, allowed region corresponds to  $R_0 > r_0 \geq r > d_1 > 0 > d_2$ , such that the function  $G(r)$  can be write as  $G_1(r) = (r - R_0)(r - r_0)(r - d_1)(r - d_2)$ , in which case, from eq. (96), we obtain the following solution for the proper time

$$\tau^{(1)}(r) = \Omega_1 \left[ F(\psi_1; \kappa_1) - \frac{R_0 - r_0}{R_0} \Pi(\psi_1; \kappa_1, n_1) \right], \quad (99)$$

where

$$\Omega_1 = \frac{\lambda}{m} \frac{2R_0}{\sqrt{(R_0 - d_1)(r_0 - d_2)}}, \quad \psi_1 = \arcsin \sqrt{\frac{(r_0 - r)}{n_1(R_0 - r)}}, \quad \kappa_1 = \sqrt{n_1 \frac{(R_0 - d_2)}{(r_0 - d_2)}}, \quad \text{and} \quad n_1 = \frac{r_0 - d_1}{R_0 - d_1}.$$

On the other hand, in the coordinate time framework the general solution corresponds to

$$t^{(1)}(r) = A_1 t_I(r) + A_2 t_{II}(r) + A_3 t_{III}(r) + A_4 t_{IV}(r), \quad (100)$$

the divergent solution at the event horizon is  $t_{II}$ , which is given by

$$t_{II}(r) = (r_0 - r_+) F(\psi_1; \kappa_1) + (R_0 - r_0) \Pi(\psi_1; \kappa_1, n_2), \quad (101)$$

with

$$A_2 = \frac{54}{m \lambda^6} \frac{1}{(R_0 - r_+)(r_0 - r_+) \sqrt{(R_0 - d_1)(r_0 - d_2)}}, \quad \text{and} \quad n_2 = \sqrt{\frac{R_0 - r_+}{r_0 - r_+} \frac{r_0 - d_1}{R_0 - d_1}}.$$

FIG. 12 summarizes our result in this case and shows the fall to the event horizon.

### 2. Second Kind: Fall to cosmological horizon

Now, we are considering the radial motion of particles that fall to the cosmological horizon. In this case, the radial coordinate belong to the interval  $r_{++} > r \geq R_0$ . So that, the solution for the proper time is

$$\tau^{(2)}(r) = \Omega_2 \left[ F(\psi_2; \kappa_1) + \frac{R_0 - r_0}{r_0} \Pi(\psi_2; \kappa_1, n_3) \right], \quad (102)$$

where

$$\Omega_2 = \frac{\lambda}{m} \frac{2r_0}{\sqrt{(R_0 - d_1)(r_0 - d_2)}}, \quad \psi_2 = \arcsin \sqrt{\frac{(r - R_0)}{n_3(r - r_0)}}, \quad \text{and} \quad n_3 = \frac{R_0 - d_2}{r_0 - d_2}.$$

In the coordinate time framework, after write the motion equation in terms of partial fractions, we obtain the general solution

$$t^{(2)}(r) = A_1 t_I(r) + A_2 t_{II}(r) + A_3 t_{III}(r) + A_4 t_{IV}(r), \quad (103)$$

the divergent solution at the cosmological horizon is  $t_I$ , which is given by

$$t_I(r) = (r_{++} - R_0)F(\psi_2; \kappa_1) + (R_0 - r_0)\Pi(\psi_2; \kappa_1, n_4), \quad (104)$$

with

$$A_1 = \frac{54}{m\lambda^6} \frac{1}{(r_{++} - R_0)(r_{++} - r_0)\sqrt{(R_0 - d_1)(r_0 - d_2)}}, \quad \text{and} \quad n_4 = n_3 \frac{r_{++} - r_0}{r_{++} - R_0}.$$

FIG. 12 shows the behavior of the radial fall to event horizon.

### B. Radial Critical Trajectory

One important case appears when a maximum in the effective potential exists. First at all, we consider that  $E < 1$  and  $q < 1$ , then we have four real roots, where the maximum occurs at  $r = D_C$ ,

$$G_{II}(r) = (r - D_C)^2 g(r), \quad (105)$$

where

$$g(r) = (r - D_1)(r - D_2), \quad (106)$$

and the quadrature is

$$\tau(r) = \pm \frac{3}{\lambda^2} \int \frac{r}{|r - D_C| \sqrt{g(r)}} dr, \quad (107)$$

Here, we can classify orbits in terms of the distance where the trajectory starts respect to  $D_C$ . We start with critical first kind, they correspond to trajectories that asymptotically move to  $D_C$  from greater distances  $R_0$ , and the region under consideration is given by  $R_0 > r > D_C > D_1 > 0 > D_2$ . Then choosing negative sign for a fall from  $R_0$ , we obtain

$$\tau(r) = -\frac{3}{\lambda^2} \int_{R_0}^r \left[ 1 + \frac{D_C}{(r - D_C)} \right] \frac{dr}{\sqrt{g(r)}}, \quad (108)$$

whose general solution is

$$\tau(r) = \frac{3}{\lambda^2} [\tau_I(r) + \tau_{II}(r)], \quad (109)$$

where the first integral is a regular function

$$\tau_I(r) = \ln \left[ \frac{D_C + R_0 + \sqrt{g(R_0)}}{D_C + r + \sqrt{g(r)}} \right], \quad (110)$$

second integral is divergent at  $D_C$

$$\tau_{II}(r) = \frac{1}{\sqrt{2}} \ln \left[ \frac{R_0 - D_C}{r - D_C} \right] - \frac{1}{\sqrt{2}} \ln \left[ \frac{4R_0 + 2\sqrt{2}\sqrt{g(R_0)}}{4r + 2\sqrt{2}\sqrt{g(r)}} \right], \quad (111)$$

Then, the final solution is given by

$$\frac{\lambda^2}{3} \tau_1^{(c)}(r) = \ln \left[ \frac{D_C + R_0 + \sqrt{g(R_0)}}{D_C + r + \sqrt{g(r)}} \right] + \frac{1}{\sqrt{2}} \ln \left[ \frac{R_0 - D_C}{r - D_C} \right] - \frac{1}{\sqrt{2}} \ln \left[ \frac{4R_0 + 2\sqrt{2}\sqrt{g(R_0)}}{4r + 2\sqrt{2}\sqrt{g(r)}} \right], \quad (112)$$

The other kind corresponds to critical second kind trajectories where particles approximate to critical radios from distances less than  $D_C$  and take infinite time to reach that distance.

If the particle starts at  $r_0$  and we choose minus sign, the solution is given by

$$\frac{\lambda^2}{3} \tau_2^{(c)}(r) = \ln \left[ \frac{D_C + r_0 + \sqrt{g(r_0)}}{D_C + r + \sqrt{g(r)}} \right] + \frac{1}{\sqrt{2}} \ln \left[ \frac{D_C - r_0}{D_C - r} \right] - \frac{1}{\sqrt{2}} \ln \left[ \frac{4r_0 + 2\sqrt{2}\sqrt{g(r_0)}}{4r + 2\sqrt{2}\sqrt{g(r)}} \right], \quad (113)$$

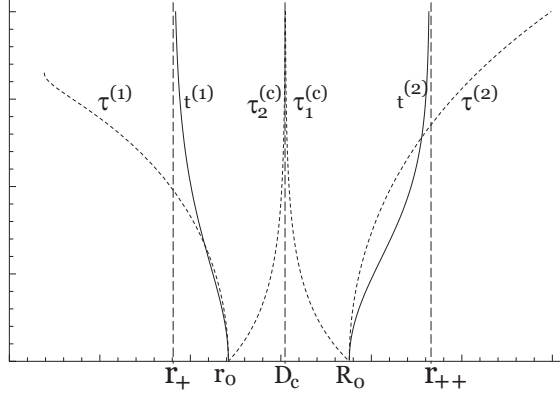


FIG. 12: Radial motion for charged particles in the coordinate time,  $t$ , and proper time,  $\tau$  with  $m = 0.1$ ,  $M = 1$ ,  $Q = 0.8$ ,  $q = 0.01$ ,  $\Lambda = 400M$

## VII. FINAL REMARKS

In this paper we studied in detail the motion of charged particles in the vicinity of the Reissner-Nordström (Anti)-dex Sitter black hole. We found, in the AdS case that exist different kinds of trajectories depending on the angular momentum of the particles. Specifically we found that exist

- **Planetary Orbit:** In this case the orbit corresponds to a bounded trajectory that exhibit oscillation between two extremal distance (periastron and apastron). Besides, this trajectory have one particular solution called Reissner-Nordström limit.
- **Second Kind Trajectory:** This trajectory is computed with the same parameter than planetary orbits. It corresponds to a trajectory that starts at rest from a finite distance less than periastron. This kind of motion represents the fall to the event horizon, and it is considered that have a turning point inside to cauchy horizon. Also it is shown an approximated solution called Reissner-Nordström limit
- **Critical Trajectories:** There are trajectories of the first and second kind. The first one, starts at rest from a finite distance from the outside of the unstable circular orbit and then approximates asymptotically to it. The second kind approximates to the unstable orbit from a distance at the inner side of it.
- **Radial Trajectory:** This trajectory has vanishing angular momentum and physically describes a radial fall to the event horizon starting at rest.
- **Circle Orbits:** For some fixed values of the constants it is possible to find solutions of the equation of motion that represent stable and unstable circle orbits.

In the dS case we mainly find two branches of classification that are summed as follow

- **Orbit with angular momentum:** here we have for a specific combination of energy and angular momentum, the possibility to have planetary orbits, when the effective potential shows a minimum. Besides, we have three different kinds of orbits that depend on the energy of the particle compared with effective potential. First kind, corresponds to an orbit whose energy is less than the global maximum of the effective potential and starts at a large distance (bigger than the last root of the respective polynomial) and the particles are doomed to go to the

cosmological horizon. Second kind, are represented by orbits that start at a distance between the event horizon and the first root of the polynomial, they are doomed to fall to the event horizon. In this case the energy of the particle is also less than the global maximum of the effective potential. Third kind, corresponds to orbits whose energy is bigger than the effective potential and particles have possibilities to move to cosmological or event horizon depending on the initial conditions in the velocity.

- Radial Orbit ( $l = 0$ ) this orbit correspond to free fall to cosmological horizon or event horizon. Also, we can find the three kinds described for the orbit with angular momentum

In sum we have characterized through a specialized study all the orbits for the black holes under consideration. We left the study of photons for a future work.

### Acknowledgments

In the initial stages of this work, we benefited particularly from insights of N. Cruz. This work was supported by COMISION NACIONAL DE CIENCIAS Y TECNOLOGIA through FONDECYT Grant 1090613 (JS). This work was also partially supported by PUCV DII (JS). J. S. and M.O. wish to thank Departamento de Física of the Universidad de Tarapacá of Arica for its kind hospitality. C.L. was supported by Universidad de Tarapacá Grant 4722-09.

---

[1] S. Chandrasekhar, *The Mathematical Theory of Black Holes*, (Oxford University Press, New York, 1983).  
[2] J. M. Maldacena, *Adv. Theor. Math. Phys.* **2**, 231-252 (1998).  
[3] F. Kottler, *Annalen Physik* **56**, 410 (1918).  
[4] S.A. Hayward, T. Shirumizo and K. Nakao, *Phys. Rev. D*, **49**, 5080 (1994).  
[5] Z. Stuchlík and S. Hledík, *Phys. Rev. D*, **60**, 044006 (1999).  
[6] M. J. Jaklitsch, C. Hellaby and D.R. Matravers, *Gen. Rel. Grav.*, **21**, 941 (1989).  
[7] J. Podolsky, *Gen. Rel. Grav.*, **31**, 1703 (1999).  
[8] Z. Stuchlík and M. Calvani, *Gen. Rel. Grav.*, **23**, 507 (1991).  
[9] G. V. Kraniotis and S. B. Whitehouse, *Class. Quantum Grav.*, **20**, 4817-4835 (2003).  
[10] G. V. Kraniotis, *Class. Quantum Grav.*, **21**, 4743-4769 (2004).  
[11] N. Cruz, M. Olivares and J.R. Villanueva, *Class. Quantum Grav.*, **22**, 1167-1190 (2005).  
[12] Z. Stuchlík and S. Hledík, *Acta Phys. Slov.*, **52**, 363 (2002).  
[13] E. Hackmann, V. Kagramanova, J. Kunz and C. Lammerzahl, *Phys. Rev. D* **78**, 124018 (2008) [Erratum-ibid. **79**, 029901 (2009)].  
[14] E. Hackmann and C. Lammerzahl, *Phys. Rev. D* **78**, 024035 (2008).  
[15] E. Hackmann and C. Lammerzahl, *Phys. Rev. Lett.* **100**, 171101 (2008).  
[16] Z. Stuchlík and P. Slany, *Phys. Rev. D*, **69**, 064001 (2004).  
[17] D. Pugliese, H. Quevedo, R. Ruffini, *Phys. Rev. D* **83**, 024021 (2011).